第 43 卷 第 2 期/2023 年 1 月/光学学报 研究论文

光学学报

石墨烯超材料等离诱导透明特性和光电开关设计

周凤麒，王嘉伟，刘志敏*，张箫，刘婷，孙丽文

华东交通大学理学院，江西 南昌 330013

摘要 基于单层图案化石墨烯超材料在太赫兹波段实现了等离子诱导透明效应，利用耦合模式理论(CMT)分析了等离子诱导透明产生的机理，得到的理论结果与时域有限差分方法计算的结果高度一致。通过调节石墨烯费米能级对等离子诱导透明特性进行了动态调控，并实现了多模同步异步开关的设计，在2.16、3.01、3.84 THz三个频率处的振幅调制度分别为95.77%、83.42%、95.58%，消光比最高可达13.73 dB。对慢光效应的研究结果表明群折射率可达180。本研究为设计光电子器件提供方案和指导。

关键词 材料；表面等离子体；石墨烯；等离子诱导透明；电光开关

中图分类号 O436 **文献标志码** A **DOI**：10.3788/AOS221115

1 引 言

表面等离子体激元(SPPs)是由入射光子和材料表面电子相互作用所产生的[1]，它是电介质与导电材料界面上价电子的集体振荡模式，在纳米尺度实现电子学与光子学的结合中起着关键作用[2-3]。由于SPPs独特的光学特性以及SPPs材料的小型化，国内外众多研究者展开了一系列科学研究[4-6]，但其受限于金属材料只能通过改变几何参数来进行静态调控[7]，所以寻找一种能够进行动态调控的SPPs材料代替金属势在必行。近年来，石墨烯作为一种具有优异电磁性能的二维材料受到研究者的广泛关注，研究表明可以通过外加栅极电压的方法来进行石墨烯[1]费米能级的动态调控[8-9]。

等离子诱导透明(PIT)现象是SPPs众多研究领域中的一个分支，PIT是法诺共振[10]的一个特例，是一种类电磁诱导透明(EIT)[7,11]现象，是由两个模式与入射光的近场耦合[12]所产生的一种异常透射现象。一个模式与入射光反应迅速且具有较大辐射损失，被称为明模式；另一个模式具有较小的辐射损失，与入射光几乎没有相互作用，被称为暗模式。明模式在暗模式与入射光相互作用激发后导致透射率急剧升高，该现象称为PIT效应。

将石墨烯和SPPs以及PIT结合起来开展研究与设计非常必要且很有研究价值。至今，在石墨烯超材料中实现PIT效应已有很多报道[13-25]，并且研究者设计了相关应用，如光开关[13-14,22,24-25]、多通道滤波器[20]、慢光[15-16,18,21]、传感[19,23]、吸收器[17]等。构建的方式主要是采用类EIT的明暗模式机理，但是对于石墨烯来说，PIT比EIT更具有可行性和现实意义，EIT是采用一束强泵浦光遏制材料本身对于探测光的吸收作用，在实验层面通常需要极端的实验条件才可以实现[26-28]，如超强泵浦激光、超低温等；而PIT是由材料结构本身明暗模式之间耦合作用产生的异常透射现象，可由一束入射光直接激发产生。随着研究的不断深入，大多数研究工作往结构更为复杂的单层和多层石墨烯方向发展，复杂的结构的确能带来更加奇异的特性和丰富的调控手段，但是复杂结构带来的是实验上难于实现、应用上难于设计等不利因素。因此，具有更加优异性能且结构简单的单层石墨烯超材料仍然有研究的必要。

本文提出了一种简单的周期型单层图案化石墨烯超材料结构，可在太赫兹波段范围实现动态可调PIT效应，耦合模式理论(CMT)推导计算拟合结果与时域有限差分方法(FDTD)模拟结果高度一致。相比于金属材料的EIT，石墨烯超材料可以通过外加栅极电压调控石墨烯费米能级，实现PIT效应的动态可调，因此设计了多模同步异步光电开关，此外根据群折射率随费米能级的变化研究了其慢光效应，希望通过该研究为微纳光电子及其应用提供方案和指导。

2 结构和模型设计

设计的周期型石墨烯超材料结构单元如图1所

收稿日期：2022-05-13；**修回日期**：2022-06-14；**录用日期**：2022-07-11；**网络首发日期**：2022-07-21

基金项目：国家自然科学基金(12164018，11847026，61764005，11804093)、江西省自然科学基金(20224ACB201008，20202BABL201019，20202ACBL212005)、江西省教育厅科学基金(GJJ210603)

通信作者：*liuzhimin2006@163.com

示，图 1(a)是三维结构图，单层石墨烯夹在一层硅和二氧化硅衬底之间，其中石墨烯由两部分组成，分别是4个相同大小的长方形石墨烯块和1个石墨烯长条，详细几何参数如图 1(b)所示，其中 $a=4\ \mu m$，$L_1=3.6\ \mu m$，$L_2=1.6\ \mu m$，$L_3=0.4\ \mu m$，$L_4=0.6\ \mu m$，$L_5=1.2\ \mu m$，$d_1=d_2=0.2\ \mu m$。结构中石墨烯块和石墨烯条可以利用化学气相沉积法[29]生长在铜箔上，然后通过干法和湿法转移技术将其转移至平坦的硅基衬底上。本文在进行实际仿真模拟和计算过程中，通过添加连续性边界条件计算并配合单元计算结果，可以得到准确的周期型超材料透射谱线。石墨烯费米能级的调节可通过在石墨烯层添加电极调控外加栅极电压来实现[8-9]，其中用于调节费米能级必备的偏置源和偏置线尺寸很小，对材料本身的光特性影响可以忽略不计[30]。

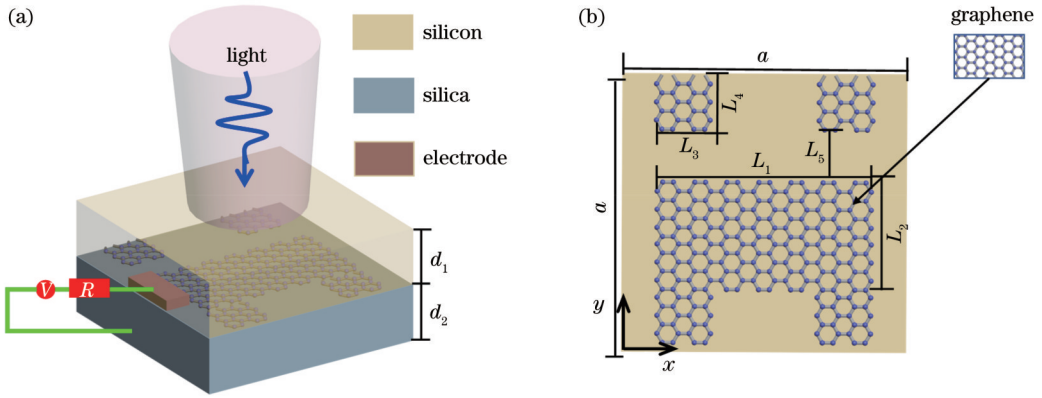

图 1　超材料结构单元示意图。(a)三维结构图；(b)俯视图

Fig. 1　Schematic diagrams of metamaterial structural unit. (a) 3D structure; (b) overhead view

当光场沿 z 方向垂直入射到所设计的结构材料中时，可以明显地观察到 PIT 效应，如图 2(a)所示。为更加清楚地了解 PIT 透明窗口的形成过程和机理，分别研究了不同结构的共振响应情况，结果表明：4个相同的长方形石墨烯块在 1～5 THz 范围内不与入射光相互作用，如图 2(a)中点划线所示，也没有形成局域光场，如图 2(b)所示，称之为暗模式；长条石墨烯与入射光作用后形成了一个透射谷，透射谷频率 $f=2.89$ THz，如图 2(a)中虚线所示，在长条石墨烯附件出现局域光场，如图 2(d)所示，称之为明模式；当暗模式被明模式和入射光相互作用的光场激发时，透射谷所对应频率处会出现异常透射现象，如图 2(a)中实线所示，频率 $f=2.85$ THz 透射峰的场分布结果显示局域光场消失，如图 2(c)所示，该现象为 PIT 效应。同时也给出了频率分别为 f_1(1.98 THz)和 f_2(3.69 THz)两个透射谷的场分布，显示在明暗模式结构上即出现强的局域场分布，如图 2(e)、(f)所示。

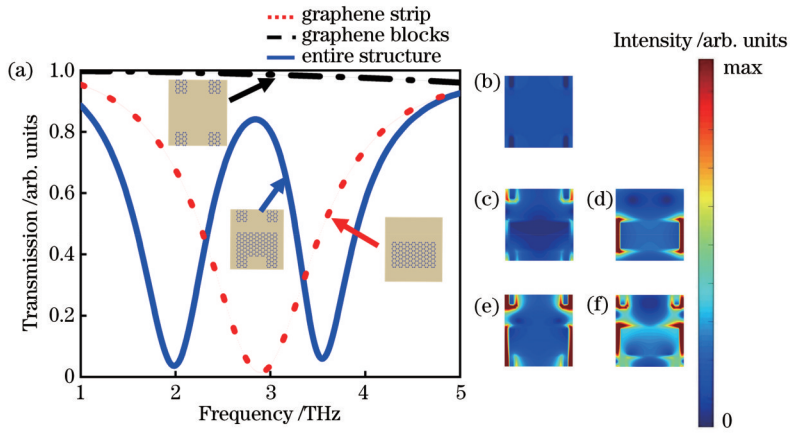

图 2　石墨烯超材料结构透射谱线及各频率点处电场分布。(a)透射谱线；(b)暗模式电场分布图；(c)整体结构透射峰处电场分布图；(d)明模式透射谷处电场分布图；整体结构(e)f_1和(f)f_2处电场分布图

Fig. 2　Transmission spectra of graphene metamaterial structure and electric field distributions at different frequencies. (a) Transmission spectra; (b) electric field distribution of dark mode; (c) electric field distribution of entire structure at transmission peak; (d) electric field distribution of bright mode at transmission dip; electric field distributions of entire structure at (e) f_1 and (f) f_2

3　理论研究方法

为了进一步揭示PIT产生的物理机理，采用CMT方法[3,7]进行理论计算，图3便于理解CMT的能量传递关系，图中上标“in/out”表示能量的流动方向，下标“+/−”表示平面光的传播方向（假定入射光传播方向为正方向），A_1和A_2是两个模式的振幅，μ_{12}和μ_{21}表示两个模式之间的耦合系数，且$\mu_{12}=\mu_{21}=1.1\times10^{11}$，$\gamma_{in}$和$\gamma_{on}(n=1,2)$分别表示它们的内部损耗系数和外部损耗系数。

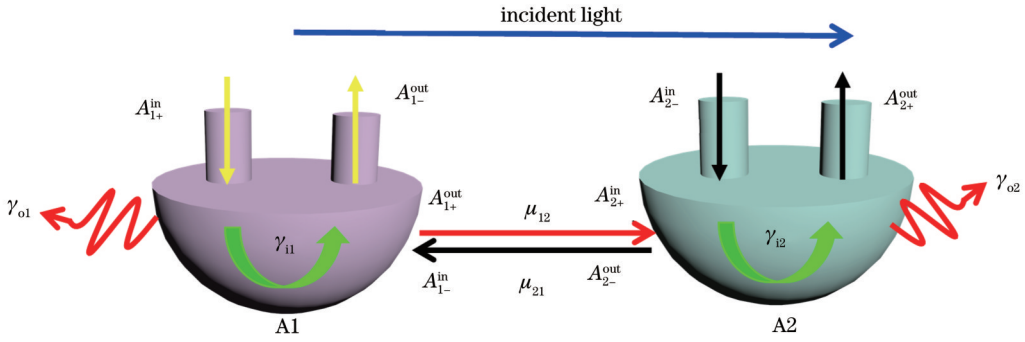

图3　CMT模型

Fig. 3　Model based on CMT

石墨烯的电导率σ由带内电子和光子发生碰撞散射σ_{intra}和带间电子跃迁σ_{inter}两部分组成[31-32]：

$$\sigma_{inter}=\frac{ie^2(\omega+i\tau^{-1})}{4\pi k_B T}\int_0^{+\infty}\frac{G(\xi)}{\hbar^2(\omega+i\tau^{-1})/(2k_B T)^2-\xi^2},\tag{1}$$

$$\sigma_{intra}=\frac{2ie^2k_B T}{\pi\hbar^2(\omega+i\tau^{-1})}\ln\left[2\cosh\left(\frac{E_F}{2k_B T}\right)\right],\tag{2}$$

式中：i为虚数单位；e、E_F、ω、$\hbar$分别为电子电荷量、石墨烯的费米能级、入射光的角频率、约化普朗克常数；$\mu=1\ m^2/(V\cdot s)$为石墨烯的迁移率；$V_F=10^6\ m/s$为费米载流子速度，$\tau=\mu E_F/(eV_F^2)$为载流子弛豫时间；$G(\xi)=\sinh\xi/[\cosh(E_F/k_B T)+\cosh\xi]$，$\xi=\varepsilon/(k_B T)$，其中$\varepsilon$、$k_B$、$T$分别为石墨烯相对介电常数、玻尔兹曼常数、环境温度。由于石墨烯电导率在太赫兹波段主要受带内σ_{intra}影响，所以可以忽略σ_{inter}，另外仿真条件下$T=300\ K$，所以有$E_F\gg k_B T$。对公式进行进一步简化，由Kubo公式可知石墨烯的电导率σ为

$$\sigma=\frac{ie^2E_F}{\pi\hbar^2(\omega+i\tau^{-1})}。\tag{3}$$

由于材料上下所使用的衬底不同，所以石墨烯的传播常数公式可以表示为

$$\frac{\varepsilon_{rSi}}{\sqrt{\beta^2-\varepsilon_{rSi}k_0^2}}+\frac{\varepsilon_{rSiO2}}{\sqrt{\beta^2-\varepsilon_{rSiO2}k_0^2}}=-\frac{i\sigma}{\omega\varepsilon_{r0}},\tag{4}$$

式中：β为传播常数；k_0为波数；ε_{rSi}、ε_{rSiO2}、ε_{r0}分别是硅的相对介电常数、二氧化硅的相对介电常数、空气的相对介电常数。在CMT中石墨烯明暗模式分别对应如图3所示的谐振器A1和A2，它们之间存在的关系[33]为

$$\begin{pmatrix}\gamma_1 & -i\mu_{12}\\ -i\mu_{21} & \gamma_2\end{pmatrix}\cdot\begin{pmatrix}a_1\\ a_2\end{pmatrix}=\begin{pmatrix}-\gamma_{o1}^{1/2} & 0\\ 0 & -\gamma_{o2}^{1/2}\end{pmatrix}\cdot\begin{pmatrix}A_{1+}^{in}+A_{1-}^{in}\\ A_{2+}^{in}+A_{2-}^{in}\end{pmatrix},\tag{5}$$

式中：$\gamma_n=i\omega-i\omega_n-\gamma_{in}-\gamma_{on}(n=1,2)$，其中$\omega_n$为第$n$个共振角频率；$\gamma_{in}$和$\gamma_{on}$由$\gamma_{in}=\omega_n/(2q_{in})$和$\gamma_{on}=\omega_n/(2q_{on})$分别得出，其中内部损耗品质因子$q_{in}=\mathrm{Re}(n_{eff})/\mathrm{Im}(n_{eff})$可以通过有效折射率$n_{eff}=\beta/k_0$得到，外部损耗因子$q_{on}$可以通过$1/q_n=1/q_{in}+1/q_{on}$得到，其中$q_n=f/\Delta f$是整个系统的品质因子（$\Delta f$是半峰全宽）。根据能量守恒，假设激发源能量只从一个模式的正方向入射，能量的传递表达式可以理解为

$$A_{1+}^{in}=E,\tag{6}$$

$$A_{1-}^{in}=-\gamma_{o2}^{1/2}\cdot a_2\cdot\exp(i\varphi),\tag{7}$$

$$A_{2+}^{in}=A_{1+}^{in}\cdot\exp(i\varphi)-\gamma_{o1}^{1/2}\cdot a_1\cdot\exp(i\varphi),\tag{8}$$

$$A_{2-}^{in}=0,\tag{9}$$

式中：E为入射能量；φ为A_1和A_2之间的相位差。谐振腔中入射光波和出射光波能量传递过程中的衰减和损耗满足

$$\begin{cases}A_{2+}^{in}=A_{1+}^{out}\cdot\exp(i\varphi)\\ A_{1-}^{in}=A_{2-}^{out}\cdot\exp(i\varphi)\end{cases},\tag{10}$$

$$\begin{cases}A_{1+}^{out}=A_{1+}^{in}-\gamma_{o1}^{1/2}\cdot a_1\\ A_{1-}^{out}=A_{1-}^{in}-\gamma_{o1}^{1/2}\cdot a_1\\ A_{2+}^{out}=A_{2+}^{in}-\gamma_{o2}^{1/2}\cdot a_2\\ A_{2-}^{out}=A_{2-}^{in}-\gamma_{o2}^{1/2}\cdot a_2\end{cases},\tag{11}$$

将式(10)、(11)计算结果代入式(5)中，可以得出透射系数表达式为

$$t=\frac{A_{2+}^{out}}{A_{1+}^{in}}=\exp(i\varphi)-\gamma_{o1}^{1/2}\cdot\exp(i\varphi)\cdot D_{a_1}-\gamma_{o2}^{1/2}\cdot D_{a_2},\tag{12}$$

其中系数D_{a_1}、D_{a_2}分别为

$$D_{a_1}=\frac{\gamma_2\cdot\gamma_{o1}^{1/2}+\chi_{12}\cdot\gamma_{o2}^{1/2}\cdot\exp(i\varphi)}{\chi_{12}\chi_{21}-\gamma_1\gamma_2},\tag{13}$$

$$D_{a_2}=\frac{\chi_{21}\cdot\gamma_{o1}^{1/2}+\gamma_1\cdot\gamma_{o2}^{1/2}\cdot\exp(i\varphi)}{\chi_{12}\chi_{21}-\gamma_1\gamma_2},\tag{14}$$

式中：$\chi_{12(21)}=i\mu_{12(21)}+\gamma_{o1}^{1/2}\cdot\gamma_{o2}^{1/2}\cdot\exp(i\varphi)$。

最后，由 $\bar{T}=|t|^2$ 得到透射率。

4　结果与分析

PIT 效应的动态调控可以通过外加栅极电压改变石墨烯的费米能级实现[8-9]，而不需要改变几何参数，基于这一动态调控[4]，有

$$E_F=\hbar V_F\sqrt{\frac{\pi\varepsilon_0\varepsilon_{Si}V_g}{de}},\tag{15}$$

式中：V_g、d、ε_0 分别为栅极电压、衬底厚度和空气的相对介电常数；ε_{Si} 为衬底硅的相对介电常数。通过在 0.7～1.0 eV 内调节石墨烯费米能级，得到透射谱线变化情况的结果如图 4 所示，图 4(a1)～(a4)中虚线为 CMT 理论结果，实线为 FDTD 数值计算结果，两者表现出高度的一致性。具体来看动态调控结果：随着费米能级的升高，透射谱线有明显的蓝移现象，如图 4(b)所示。透射峰和透射谷的频率显示出近似的线性关系，这也可以从图 4(c)中的三维演化图中更清楚地看到。

研究结果表明：在调节石墨烯费米能级时蓝移现象可以使得透射谷和透射峰发生重合，因此可以利用该结果来设计光电开关。利用石墨烯超材料设计光子器件已有一些报道[14,25]，但是这些关于光与石墨烯耦合所设计的器件结构都较为复杂，本文可以在一种简单的石墨烯超材料结构中设计光电开关，并通过动态调控提出实现同步和异步开关的设计。设计的方案和思路如下：选取费米能级为 0.7 eV（实线）和 1.2 eV（虚线），结果如图 5 所示，当费米能级为 0.7 eV 时，在 f_1（2.16 THz）和 f_3（3.84 THz）时处于“开”状态，而在 f_2

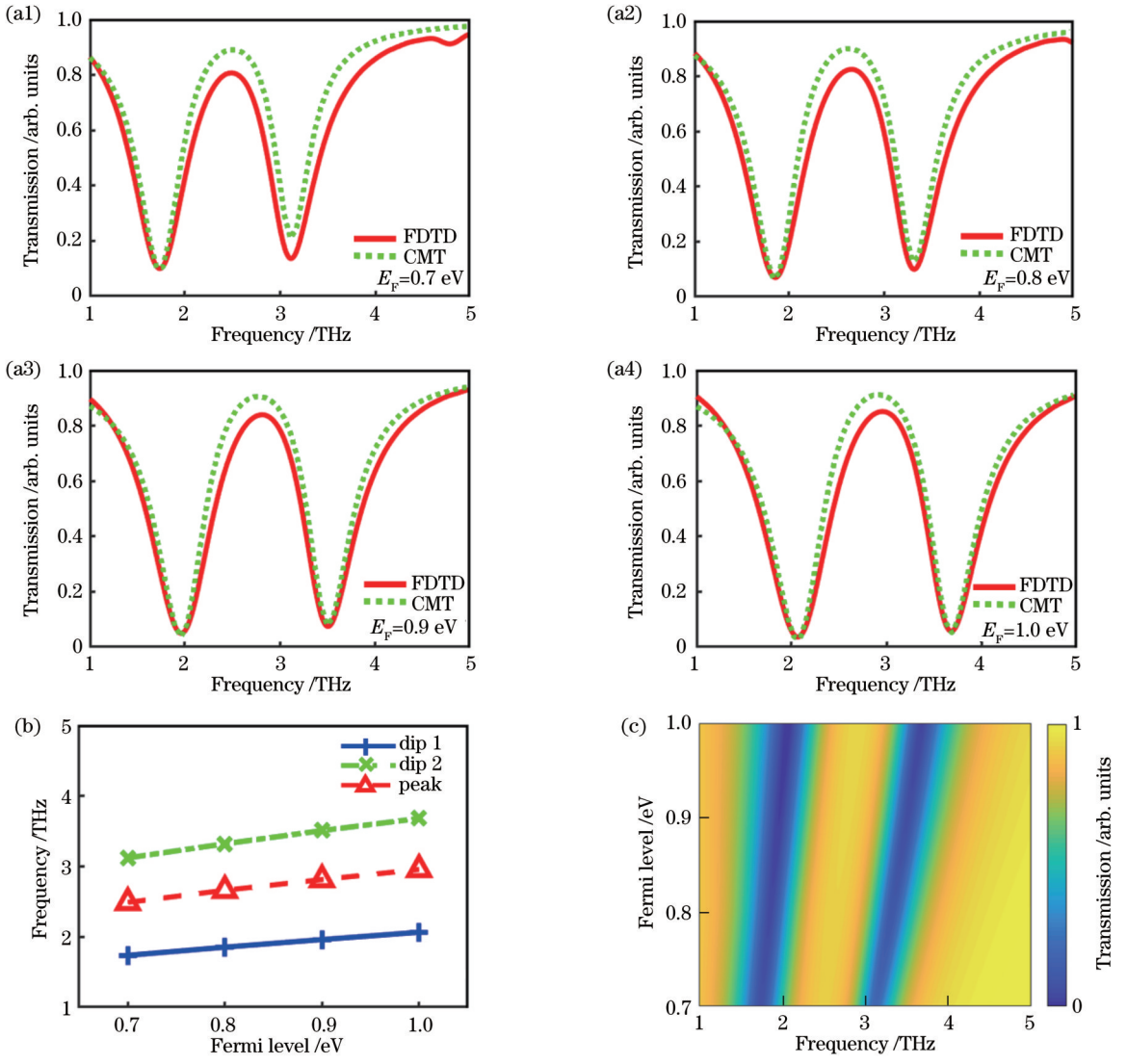

图 4　不同费米能级下材料透射谱和 PIT 的变化情况。(a1)～(a4) CMT 和 FDTD 得到不同费米能级下的透射谱；(b) PIT 透射峰和透射谷随费米能级的演化图；(c) PIT 随费米能级的三维演化图

Fig. 4　Variations of material transmission spectra and PIT at different Fermi levels. (a1)-(a4) Transmission spectra at different Fermi levels obtained by CMT and FDTD method; (b) evolution diagram of dips and peak of PIT at different Fermi levels; (c) 3D evolution diagram of PIT at different Fermi levels

(3.01 THz)时处于“闭”状态;对应地,当费米能级调节至 1.2 eV 时,f_1和f_3处同时变为“闭”状态,f_2处变成“开”状态,这就构成了三个不同频率处的同步异步开关设计。同时振幅调制度D_{MA}[4]可以用来描述其同步异步光电开关的调制能力,可通过以下方式获得:

$$D_{MA}=\frac{|A_{on}-A_{off}|}{A_{on}}\times 100\%, \tag{16}$$

式中:A_{on}、A_{off}分别为“开”“关”状态下的信号强度,在本文中为对应状态的透射率大小。因此在 2.16、3.01、3.84 THz 处可以实现的开关调制幅度分别为 95.77%、83.42%、95.58%。另外,消光比R_E和退相时间t_d也是描述光电开关特性的重要参数[25, 34-35],可以分别通过$R_E=10\times\lg(T_{on}/T_{off})$($T_{on}$、$T_{off}$分别为“开”“关”状态下的透射率)和$t_d=2\hbar/\Delta f$计算得到,由此得到三个频率处的消光比和退相时间分别是 13.73 dB、7.80 dB、13.54 dB 和 2.49、7.66、3.42 ps。从开关的设计类型、超材料结构、振幅调制度和消光比的结果来看,本文的结果具有较高的研究和应用价值,如表 1 所示,可以看出所设计的光电开关在振幅调制上具有较好的性能。

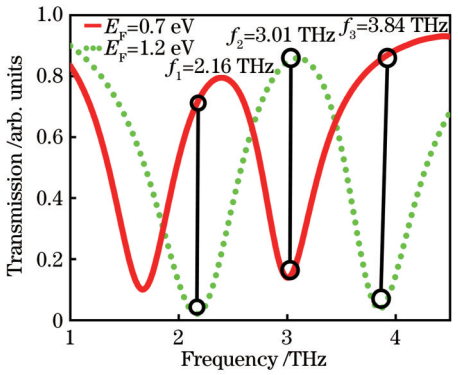

图 5　光电开关理论设计

Fig. 5　Theoretical design of photoelectric switch

表 1　不同石墨烯超材料光电开关对比

Table 1　Comparison of photoelectric switches with different graphene metamaterials

Type of switch	Metamaterial structure	Amplitude modulation degree D_{MA} /%	Extinction ratio R_E /dB
Quadruple state photoelectric switch[24]	Three-layer structure	74.7, 87.8, 76.5, 77.7	5.97, 9.15, 6.30, 6.51
Single state photoelectric switch[14]	Three-layer structure	83.3	7.77
Dual state photoelectric switch[25]	Double-layer structure	67.5, 86.1, 65.3	4.89, 8.58, 4.60
Synchronous asynchronous photoelectric switch (this article)	Single layer structure	95.77, 83.42, 95.58	13.73, 7.80, 13.54

利用 PIT 设计的光电开关可应用于光电子领域,此外,慢光特性也是 PIT 应用的一个重要方面,通常用群折射率来评判一个材料的慢光特性,群折射率n_g[17]可表示为

$$n_g=c\frac{\mathrm{d}k_0}{\mathrm{d}\omega}=\frac{c}{h}\frac{\mathrm{d}\theta}{\mathrm{d}\omega}, \tag{17}$$

式中:c、θ、h分别是真空中的光速、相移角、衬底的厚度。选取 0.7~1.0 eV 费米能级绘制群折射率和相移随着频率的变化曲线,如图 6 中实线所示,群折射率最

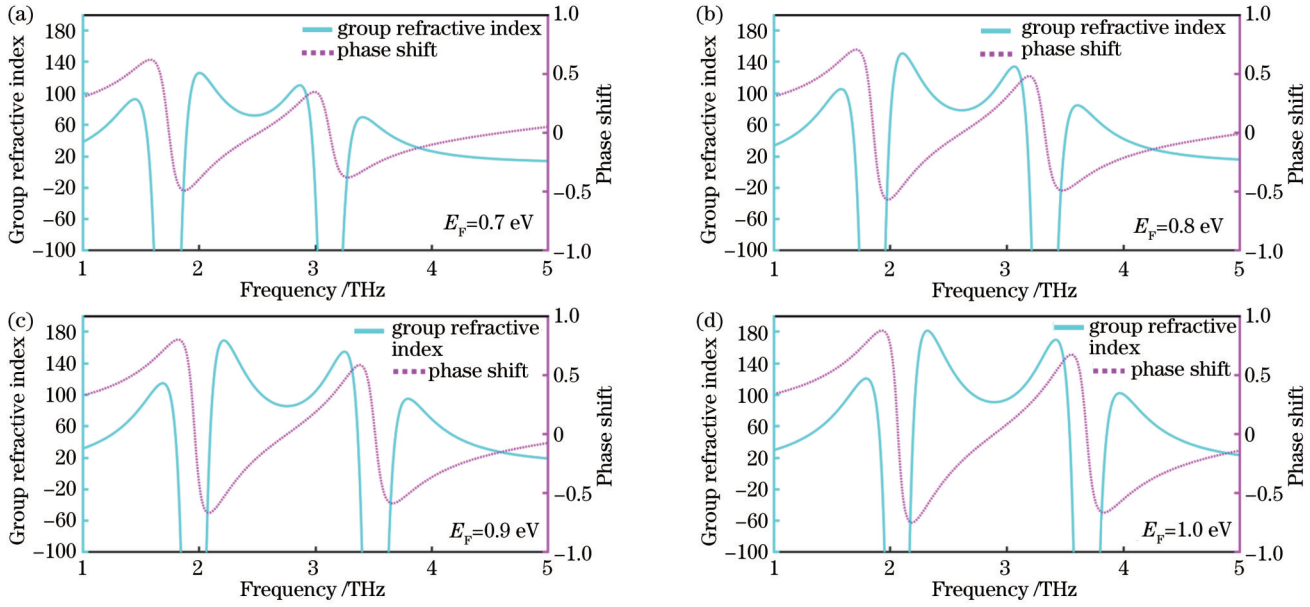

图 6　不同费米能级下的群折射率和相移。(a) E_F=0.7 eV;(b) E_F=0.8 eV;(c) E_F=0.9 eV;(d) E_F=1.0 eV

Fig. 6　Group refractive index and phase shift at different Fermi levels. (a) E_F=0.7 eV; (b) E_F=0.8 eV; (c) E_F=0.9 eV; (d) E_F=1.0 eV

高可达180，这为在单层的简单超材料结构中实现高群折射率，从而实现优异慢光效应提供方案和指导。

5 结 论

提出了一种简单的单层图案化石墨烯超材料结构，并实现了PIT效应，该现象是由明暗模式之间的相消干涉产生的。通过改变石墨烯费米能级可在2.16、3.01、3.84 THz处实现开关调制，由此提出了多模同步异步开关的设计，振幅调制度、消光比和群折射率最高可分别达95.77%、13.73 dB和180。本文研究结果可为太赫兹石墨烯等离激元器件的设计提供指导。

参 考 文 献

[1] Barnes W L, Dereux A, Ebbesen T W. Surface plasmon subwavelength optics[J]. Nature, 2003, 424(6950): 824-830.

[2] Xia S X, Zhai X, Wang L L, et al. Excitation of surface plasmons in graphene-coated nanowire arrays[J]. Journal of Applied Physics, 2016, 120: 103104.

[3] Xia S X, Zhai X, Huang Y, et al. Graphene surface plasmons with dielectric metasurfaces[J]. Journal of Lightwave Technology, 2017, 35(20): 4553-4558.

[4] Fei Z, Rodin A S, Andreev G O, et al. Gate-tuning of graphene plasmons revealed by infrared nano-imaging[J]. Nature, 2012, 487(7405): 82-85.

[5] Liu Z Q, Liu G Q, Zhou H Q, et al. Near-unity transparency of a continuous metal film via cooperative effects of double plasmonic arrays[J]. Nanotechnology, 2013, 24(15): 155203.

[6] He X Y, Gao P Q, Shi W Z. A further comparison of graphene and thin metal layers for plasmonics[J]. Nanoscale, 2016, 8(19): 10388-10397.

[7] Cao G T, Li H J, Deng Y, et al. Plasmon-induced transparency in a single multimode stub resonator[J]. Optics Express, 2014, 22(21): 25215-25223.

[8] Vakil A, Engheta N. Transformation optics using graphene[J]. Science, 2011, 332(6035): 1291-1294.

[9] 姚刚. 基于石墨烯等离子体诱导透明的太赫兹超材料动态调制特性研究[D]. 武汉: 华中科技大学, 2017.
Yao G. Research on dynamic modulation characteristics of terahertz metamaterals based on graphene plasmon induced transparency[D]. Wuhan: Huazhong University of Science and Technology, 2017.

[10] Fofang N T, Grady N K, Fan Z Y, et al. Plexciton dynamics: exciton-plasmon coupling in a J-aggregate-Au nanoshell complex provides a mechanism for nonlinearity[J]. Nano Letters, 2011, 11(4): 1556-1560.

[11] Totsuka K, Kobayashi N, Tomita M. Slow light in coupled-resonator-induced transparency[J]. Physical Review Letters, 2007, 98(21): 213904.

[12] Xia S X, Zhai X, Wang L L, et al. Plasmonically induced transparency in double-layered graphene nanoribbons[J]. Photonics Research, 2018, 6(7): 692.

[13] Zhang X, Liu Z M, Zhang Z B, et al. Polarization-sensitive triple plasmon-induced transparency with synchronous and asynchronous switching based on monolayer graphene metamaterials[J]. Optics Express, 2020, 28(24): 36771-36783.

[14] Zhang X, Liu Z M, Zhang Z B, et al. Photoelectric switch and triple-mode frequency modulator based on dual-PIT in the multilayer patterned graphene metamaterial[J]. Journal of the Optical Society of America A, Optics, Image Science, and Vision, 2020, 37(6): 1002-1007.

[15] Xie Y Y, Chai J X, Ye Y C, et al. A tunable slow light device with multiple channels based on plasmon-induced transparency [J]. Plasmonics, 2021, 16(5): 1809-1816.

[16] Xiong C X, Xu H, Zhao M Z, et al. Triple plasmon-induced transparency and outstanding slow-light in quasi-continuous monolayer graphene structure[J]. Science China Physics, Mechanics & Astronomy, 2021, 64(2): 224211.

[17] Gao E D, Liu Z M, Li H J, et al. Dynamically tunable dual plasmon-induced transparency and absorption based on a single-layer patterned graphene metamaterial[J]. Optics Express, 2019, 27(10): 13884-13894.

[18] Ruan B X, Xiong C X, Liu C, et al. Tunable plasmon-induced transparency and slow light in a metamaterial with graphene[J]. Results in Physics, 2020, 19: 103382.

[19] Cui W, Li C J, Ma H Q, et al. Excellent sensing based on dual-plasmon induced transparency in graphene metasurface[J]. Physica E: Low-Dimensional Systems and Nanostructures, 2021, 134: 114850.

[20] Liu Z M, Gao E D, Zhang X, et al. Terahertz electro-optical multi-functional modulator and its coupling mechanisms based on upper-layer double graphene ribbons and lower-layer a graphene strip[J]. New Journal of Physics, 2020, 22(5): 053039.

[21] Liu Z M, Gao E D, Li H J, et al. Investigation of plasmon-induced transparency and reflection in patterned graphene metamaterial[J]. Journal of Applied Physics, 2019, 126(12): 123101.

[22] Liu Z M, Zhang X, Zhou F Q, et al. Triple plasmon-induced transparency and optical switch desensitized to polarized light based on a mono-layer metamaterial[J]. Optics Express, 2021, 29(9): 13949-13959.

[23] Ge J H, You C L, Feng H, et al. Tunable dual plasmon-induced transparency based on a monolayer graphene metamaterial and its terahertz sensing performance[J]. Optics Express, 2020, 28(21): 31781-31795.

[24] Liu Z M, Zhang X, Zhang Z B, et al. Simultaneous switching at multiple frequencies and triple plasmon-induced transparency in multilayer patterned graphene-based terahertz metamaterial[J]. New Journal of Physics, 2020, 22(8): 083006.

[25] Zhou F Q, Wang Y Q, Zhang X J, et al. Dynamically adjustable plasmon-induced transparency and switching application based on bilayer graphene metamaterials[J]. Journal of Physics D: Applied Physics, 2021, 54(5): 054002.

[26] 王子煜, 邵健, 胡亚新, 等. 基于全介质超材料的高Q电磁诱导透明现象研究[J]. 光学学报, 2021, 41(11): 1116001.
Wang Z Y, Shao J, Hu Y X, et al. Electromagnetically induced transparency based on all-dielectric metamaterial with high Q factor[J]. Acta Optica Sinica, 2021, 41(11): 1116001.

[27] 张敏, 延凤平, 杜雪梅, 等. 太赫兹多波段的电磁诱导透明设计与分析[J]. 中国激光, 2021, 48(3): 0314001.
Zhang M, Yan F P, Du X M, et al. Design and analysis of electromagnetically induced transparency in THz multiband[J]. Chinese Journal of Lasers, 2021, 48(3): 0314001.

[28] 李洪阳, 黄巍, 张玉婷, 等. 基于锑化铟太赫兹超材料可调谐的电磁感应透明[J]. 激光与光电子学进展, 2021, 58(5): 0530002.
Li H Y, Huang W, Zhang Y T, et al. Tunable electromagnetically induced transparency based on indium antimonide terahertz metamaterial[J]. Laser & Optoelectronics Progress, 2021, 58(5): 0530002.

[29] Suk J W, Kitt A, Magnuson C W, et al. Transfer of CVD-grown monolayer graphene onto arbitrary substrates[J]. ACS Nano, 2011, 5(9): 6916-6924.

[30] Cheng H, Chen S Q, Yu P, et al. Dynamically tunable plasmonically induced transparency in periodically patterned graphene nanostrips[J]. Applied Physics Letters, 2013, 103(20): 203112.

[31] Falkovsky L A. Optical properties of graphene[J]. Journal of Physics: Conference Series, 2008, 129: 012004.

[32] Falkovsky L A, Pershoguba S S. Optical far-infrared properties

of a graphene monolayer and multilayer[J]. Physical Review B, 2007, 76(15): 153410.
[33] Fan S H, Suh W, Joannopoulos J D. Temporal coupled-mode theory for the Fano resonance in optical resonators[J]. Journal of the Optical Society of America A, Optics, Image Science, and Vision, 2003, 20(3): 569-572.
[34] Zhang X, Zhou F Q, Liu Z M, et al. Quadruple plasmon-induced transparency of polarization desensitization caused by the Boltzmann function[J]. Optics Express, 2021, 29(18): 29387-29401.
[35] Ahmadivand A, Sinha R, Gerislioglu B, et al. Transition from capacitive coupling to direct charge transfer in asymmetric terahertz plasmonic assemblies[J]. Optics Letters, 2016, 41(22): 5333-5336.

Plasmon-Induced Transparency Effect and Photoelectric Switch Design Based on Graphene Metamaterial

Zhou Fengqi, Wang Jiawei, Liu Zhimin*, Zhang Xiao, Liu Ting, Sun Liwen
School of Science, East China Jiaotong University, Nanchang 330013, *Jiangxi, China*

Abstract

Objective Surface plasma polaritons (SPPs) have been greatly promoted in recent years in the field of nano-photonology. There have been many studies which show that the SPPs can be generated on the surface of graphene and dielectric, and plasma induced transparency (PIT) effect due to the interaction between the incident light and the structure as an abnormal transmission phenomenon has been studied generally. With the advantage of dynamic modulation, the graphene has greater advantages than the precions metal materials in PIT effect, which has been proven to play a key role in the next generation of photonic devices such as photoelectric switches, sensors, and slow-light devices. The PIT effect based on patterned graphene metamaterials has evolved towards multi-layered complex structures that can achieve very excellent electromagnetic properties. However, complex patterned graphene is difficult to be produced and put into use limited by the development of nanomanufacturing technology. It is very significant to study the simple structure and high quality PIT effect for the manufacture and application of PIT devices in experiment and real life. At the same time, designing simple, manufacturable structures to produce high-quality multi-mode PIT is of great significance to the development of the SPPs field. It will also greatly promote the rapid development and application of photonic devices based on PIT effect.

Methods In this paper, the PIT effect of monolayer patterned graphene metamaterials is studied by combining numerical simulation of electromagnetic field via finite-difference time-domain (FDTD) and theoretical calculation via coupled-mode theory (CMT). We design a single-layer metamaterial structure composed of graphene blocks and graphene strips, use FDTD solution for electromagnetic field simulation calculations to observe the transmission and power field local, and thus analyze the interaction between the light-dark mode and the incident light. Next, by deducing the theoretical formula of graphene surface conductivity, the effect of gate voltage applied changing with the Fermi level of graphene on the dielectric constant of graphene is obtained. By studying the effect of different Fermi level graphene on the PIT effect, the relevant application design scheme is proposed. CMT is widely regarded as two or more time model and spatial coupling electromagnetic wave general law of the most effective theory in recent years. In this paper, the structures of bright and dark models are used as two resonators for the analysis of mode coupling effect, through rigorous formula derived theoretical material transmittance formula. Finally, we compare numerical simulation results and theoretical calculation results to verify the rationality and correctness of the simulation calculation.

Results and Discussions In this paper, a simple monolayer patterned graphene metamaterial is designed to achieve high quality PIT effect (Figs. 1 and 2). By changing the size of the gate voltage to dynamically regulate the Fermi level of graphene, we find that with the increase of Fermi level, the PIT spectral pattern has an obvious blue shift phenomenon, and the resonance effect of each resonance point is also significantly enhanced. Meanwhile, the simulation results obtained by FDTD are highly consistent with the theoretical calculation results obtained by CMT (Fig. 4). Dynamic adjustment of the PIT spectrum is realized by adjusting the Fermi level of graphene, multimode synchronous and asynchronous switches can be designed at the frequencies of 2.16, 3.01, and 3.84 THz, the amplitude modulations of three frequencies are 95.77%, 83.42%, and 95.58%, respectively, and the extinction ratio is up to 13.73 dB (Fig. 5). Through cross-sectional comparison with different kinds of metamaterial photoelectric switches, it is found that the switch designed can realize a high amplitude modulation system with a simpler structure (Table 1). Finally, by calculating the group refractive index, we obtain the slow light characteristics of materials at different Fermi energy levels. The materials can achieve the highest

group refractive index of 180 (Fig. 6) which provides a new scheme and guidance for simple slow light devices.

Conclusions In this paper, we propose a simple graphene metamaterial structure to achieve high quality PIT effect. The dynamic tuning of PIT effect is achieved by using the properties of graphene with applied gate voltage to change the Fermi level. By analyzing the PIT effect at different Fermi levels, it is not difficult to find that as the Fermi level of graphene increases, PIT effect has obvious blue shift and resonance enhancement. At the same time, we also put forward the theory of a synchronous asynchronous photoelectric switch design, which can reach 95.77% in 2.16 THz switch modulation amplitude. The realization of high quality photoelectric switch with simple structure provides a new scheme and idea for the development of nano photoelectronic devices. At the end of the article, we discuss its slow light effect through calculating the group refractive index of the metamaterial. The maximum group refractive index of 180 can be achieved, which provides a scheme and guidance for the design and application of slow optical devices.

Key words materials; surface plasma; graphene; plasmon-induced transparency; optoelectronic switch